Thermal resistance analysis of Buried-Heterostructure and Shallow-Ridge lasers

V. Rustichelli,[1] F. Lemaître, H.P.M.M Ambrosius[1], H. Debregeas[2] and K.A. Williams

[1] COBRA Institute, Eindhoven University of Technology, NL 5600 MB Eindhoven, the Netherlands
[2] III-V lab, a joint lab between Nokia Bell Labs, Thalès and CEA-LETI, 1 av. A. Fresnel, 91767 Palaiseau France

In this paper we present a thermal resistance analysis of lasers with different waveguide geometries by using a finite difference thermal model. The model is able to predict temperature distribution, heat flux, and thermal resistance. In particular the analysis is focused on the comparison between Shallow-Ridge and Buried-Heterostructures lasers.

Introduction

The need for high-bandwidth-density photonic devices and circuits is driving photonic devices with lower consumption and more effective heat-sinking. Photonic integrated circuits such as the COBRA platform use either deep or shallow ridge waveguides to define active and passive photonic devices [1]. While this is sufficient to ensure optical waveguiding, a significant proportion of the charge carriers can laterally diffuse and recombine without providing optical gain thus reducing the efficiency of the device [2]. Deep etch devices improve confinement, but with a greater sensitivity to surface recombination and roughness. Buried-heterostructure (BH) lasers offer both charge carrier and photon confinement [3], [4]. Recently we have been studying the incorporation of buried hetero-structure (BH) lasers within the COBRA integration platform [5], [6]. Importantly, BH lasers are expected to enable excellent thermal performance [7], [8] enabling further performance improvements and energy efficiency. To date there has been only limited comparative work [9].

In this work, we provide the first quantitative experimental and theoretical comparison of the thermal behavior of SR and BH lasers. We propose a finite difference thermal model to predict temperature distribution, heat flux, and thermal resistance (R_{th}) inside the laser with different waveguide geometries, and use this to interpret differences in experimental data.

Heat-spreading

Heating in semiconductor lasers is an important phenomenon that compromises the performance. When injecting electrical power into a laser, part of the input electrical power will be dissipated as heat through Joule heating in the resistive p-layers, radiative absorption, and non-radiative recombination. This will have consequences on the threshold current and internal efficiency[10] as well as modulation bandwidth and performance.

In a BH laser, the active layer is embedded in InP (See Fig-1a) providing an efficient thermal dissipation because the heat can dissipate through both sides, as well as the top and the bottom of the active stripe thanks to the relatively good thermal conductivity *k* of InP (68 $Wm^{-1}K^{-1}$) [11]. The SR laser is only partially etched (See Fig-1b), and due to the relatively poor thermal conductivity of the continuous, quaternary, active layer stack (5 $Wm^{-1}K^{-1}$), the heat-sinking is primarily through the lower side of the active layer, if top side heat removal is small.

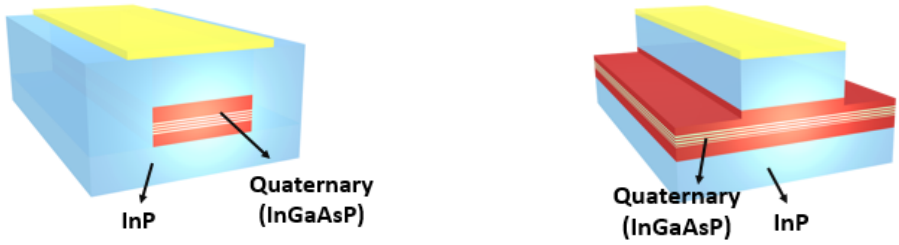

Fig.1: Cross section of (a) buried heterostructure (BH) and (b) shallow ridge (SR) laser; Red signifies the quaternary material while blue shows the higher thermal conductivity InP layers.

Numerical model

In order to obtain the two-dimensional temperature distribution cross-section of SR and BH lasers, the temperature equation below needs to be solved:

$$\frac{\partial^2 T}{\partial x^2} + \frac{\partial^2 T}{\partial y^2} = 0 \quad (1)$$

An efficient way to solve this equation is based on a finite-difference method. The spatial domain is divided in *n* nodes and, for each node, the heat flow equation is defined. For the steady state condition, the net heat flux must sum to zero at each node so:

$$q_i + \sum_j \frac{T_j - T_i}{R_{ij}} = 0 \quad (2)$$

where q_i is the heat delivered by the node *i*. When the number of nodes is large, solving the equation by directly inverting the temperature matrix it is not efficient and an iterative technique is preferred. For this work we used the so called *Gauss-Silted* method [12]. The temperature T_i is defined in terms of the thermal resistance and temperature of the adjacent nodes T_j as follow.

$$T_i = \frac{q_i + \sum_j (T_j / R_{ij})}{\sum_j (1/R_{ij})} \quad (3)$$

where R_{ij} is the thermal resistance between the node *i* and *j*. In a first step an initial value of T_i is assumed, next the new values of T_i are calculated using the updated values of T_j. The process is repeated until $\left|T_{i_{n+1}} - T_{i_n}\right| < \delta \; \forall \; T_i$, where *n* is the required number of iterations and δ is a quality of fit constant specified in this work to be 10^{-6}. A script in Matlab© was implemented to solve the temperature matrix for the laser cross-section iteratively.

The BH and SR lasers are represented as heat sources in the active core. Adiabatic boundary conditions are imposed on the side and on the top, and heat loss is only enabled via the bottom of the 100 µm thick substrate. The isothermal condition at 25 ℃ is imposed at the bottom where the device is in contact with the heat-spreader. The injected power is 160 mW and the active region width is 2 µm. Half of the space domain is used, exploiting symmetry to improve computational efficiency. Fig-2a and Fig-2b show the temperature profile for cross-sections of a BH laser and SR laser respectively.

As the heat source is embedded in InP, the heat can spread in all directions. In SR laser, the heat flux is mainly from the bottom of the active region. The effective thermal resistance of the laser is then computed by using the following relation [13]:

$$R_{th} = (T_a - T_s)/P_{in} \quad (4)$$

where T_a is the temperature in the active layer and T_s is the temperature of the substrate imposed by the cooling system, represented here by a 25°C temperature defined at the

bottom of the substrate. The calculated R_{th} for BH and SR is 24 K/W and 90 K/W respectively.

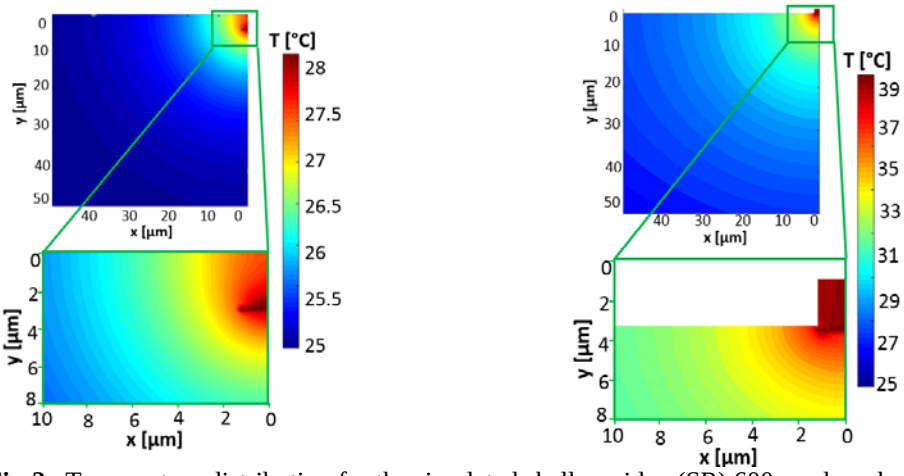

Fig-2a Temperature distribution for the simulated shallow ridge (SR) 600 µm long laser
Fig-2b Temperature distribution for the buried heterostructure (BH) 600 µm long laser

Experimental measurements

To verify the model, the thermal resistance R_{th} was experimentally measured for SR and BH lasers of varying all-active cavity lengths. Firstly, the temperature dependence of the wavelength spectrum was quantified by changing the substrate temperature at constant injected current. $\Delta\lambda/\Delta T$ was found to be 0.10 nm/K for all lasers. Secondly, by increasing the injected electrical power, the red shift of a selected longitudinal mode was measured.

The effective thermal resistance was finally estimated by using the relation below[14]:

$$R_{th} = \frac{T_a - T_s}{P_{in} - P_{opt}} \cong \frac{T_a - T_s}{Pin} = \frac{\frac{\Delta\lambda}{\Delta P_{in}}}{\frac{\Delta\lambda}{\Delta T}} \quad (5)$$

Where P_{in} is the injected electrical power and P_{opt} is the optical power, negligible respect to P_{in}. [13]

In Fig-3 the computed and measured values of thermal resistance R_{th} are plotted together. The thermal resistance is plotted as a function of laser length for experiment and theory. In the simulations, all lasers are operated with the same input electrical power levels of 160 mW. Simulations are performed in length steps of 100 µm. The increasing thermal resistance with shortened laser length corresponds to the increased input power density.

The model shows a good agreement with the measurements of BH lasers and also longer SR lasers. A deviation is noted for shorted cavity length SR lasers. This may be attributable to the assumption that heat removal is only from the bottom side electrode and a simplification in the modelled layer stacks. The model can be readily extended to include top-side cooling via the p-metal connection.

Conclusion

From both the measured values and the numerical model we can confirm the improved thermal resistance of the BH lasers respect to SR lasers. The improvement is most striking for longer devices, from order 50 K/W to 30 K/W. The enhanced heat-

spreading in the InP layers is expected to enable higher efficiency lasers, and when incorporated within integration platforms, higher performance circuits.

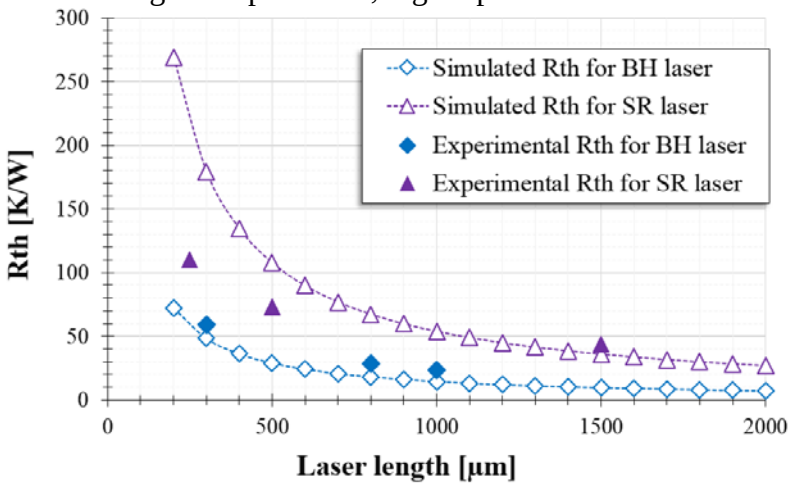

Fig 3. Thermal resistance as a function of length for BH and SR lasers. Experiment and theory.

Acknowledgements

Funding is acknowledged by the EU-project GeTPICs. The authors wish to thank for their contribution François Duport, Delphine Lanteri and Frederic Van Dijk.

References

[1] M. Smit *et al.*, "An introduction to InP-based generic integration technology," *Semicond. Sci. Technol.*, vol. 29, no. 8, p. 83001, 2014.

[2] G. J. Letal, J. G. Simmons, J. D. Evans, and G. P. Li, "Determination of Active-Region Leakage Currents in Ridge-Waveguide Strained-Layer Quantum-Well Lasers by Varying the Ridge Width," vol. 34, no. 3, pp. 512–518, 1998.

[3] C. A. Barrios, S. Lourdudoss, and H. Martinsson, "Analysis of leakage current in GaAs/AlGaAs buried-heterostructure lasers with a semi-insulating GaInP:Fe burying layer," *J. Appl. Phys.*, vol. 92, no. 5, pp. 2506–2517, 2002.

[4] C. Kazmierski *et al.*, "100 Gb/s Operation of an AlGaInAs Semi-Insulating Buried Heterojunction EML," *Opt. Fiber Commun. Conf. Natl. Fiber Opt. Eng. Conf.*, p. OThT7, 2009.

[5] V. Rustichelli, H. Ambrosius, P. J. Van Veldhoven, R. Brenot, F. Pommereau, and K. Williams, "Technology development and implementation of a transmitter in generic technology using Buried Heterostructure Semiconductor Amplifiers," pp. 43–46, 2015.

[6] K. A. Rustichelli, V.; Ambrosius, H.P.M.M.; van Veldhoven, P.J.; Brenot, R.; Williams, "Buried heterostructures for deep UV lithography," pp. 4–5, 2016.

[7] H. K. Lee, K. S. Chung, and J. S. Yu, "Thermal analysis of InP-based quantum cascade lasers for efficient heat dissipation," *Appl. Phys. B Lasers Opt.*, vol. 93, no. 4, pp. 779–786, 2008.

[8] T. Tsukada and Y. Shima, "Thermal characteristics of buried-heterostructure injection lasers," *IEEE J. Quantum Electron.*, vol. 11, no. 7, pp. 494–498, 1975.

[9] J. Jacquet *et al.*, "Thermal and optical properties of both ridge and buried structures laser including waveguide layer," vol. 8255, pp. 825527-825527–9, 2012.

[10] K. P. Pipe, R. J. Ram, and a. Shakouri, "The physics of heat transport in semiconductor lasers," *IEEE 18th Int. Semicond. Laser Conf.*, vol. 1, no. 617, pp. 77–78, 2002.

[11] J. Jacquet, Y. Abner, M. Choffla, C.-A. Paepegaey, and K. Mheidly, "Thermal dissipation in a laser and semiconductor optical amplifier," vol. 7847, p. 78470I–78470I–7, 2010.

[12] J. . Holman, "Heat transfer," p. 758, 2010.

[13] J. S. Manning, "Thermal impedance of diode lasers: Comparison of experimental methods and a theoretical model," *J. Appl. Phys.*, vol. 52, no. 5, pp. 3179–3184, 1981.

[14] T. Flick, K. H. Becks, J. Dopke, P. Mättig, and P. Tepel, "Measurement of the thermal resistance of VCSEL devices," *J. Instrum.*, vol. 6, no. 1, pp. C01021–C01021, 2011.